



HAL
open science

Intraoperative imaging for remnant viability assessment in bilateral posterior retroperitoneoscopic partial adrenalectomy in an experimental model

Barbara Seeliger, Piero Alesina, Martin K. Walz, Raoul Pop, Anne-Laure Charles, Bernard Geny, Nadia Messaddeq, George Kontogeorgos, Pietro Mascagni, Emilie Seyller, et al.

► To cite this version:

Barbara Seeliger, Piero Alesina, Martin K. Walz, Raoul Pop, Anne-Laure Charles, et al.. Intraoperative imaging for remnant viability assessment in bilateral posterior retroperitoneoscopic partial adrenalectomy in an experimental model. *British Journal of Surgery*, 2020, 10.1002/bjs.11839 . hal-03322285

HAL Id: hal-03322285

<https://hal.science/hal-03322285>

Submitted on 5 Apr 2023

HAL is a multi-disciplinary open access archive for the deposit and dissemination of scientific research documents, whether they are published or not. The documents may come from teaching and research institutions in France or abroad, or from public or private research centers.

L'archive ouverte pluridisciplinaire **HAL**, est destinée au dépôt et à la diffusion de documents scientifiques de niveau recherche, publiés ou non, émanant des établissements d'enseignement et de recherche français ou étrangers, des laboratoires publics ou privés.

Intraoperative imaging for remnant viability assessment in bilateral posterior retroperitoneoscopic partial adrenalectomy in an experimental model


B. Seeliger^{1,2,3,6} , P. F. Alesina⁶ , M. K. Walz⁶, R. Pop^{1,4}, A.-L. Charles², B. Geny², N. Messaddeq⁵, G. Kontogeorgos^{7,8}, P. Mascagni¹, E. Seyller¹, J. Marescaux^{1,3}, V. Agnus¹ and M. Diana^{1,2,3} 

¹IHU-Strasbourg, Institute of Image-Guided Surgery, ²Institute of Physiology, EA3072 'Mitochondria, Oxidative Stress and Muscle Protection', Translational Medicine Federation, Faculty of Medicine, University of Strasbourg, ³Institute for Research against Digestive Cancer (IRCAD),

⁴Department of Interventional Radiology, Strasbourg University Hospitals, and ⁵Institute of Genetics and Molecular and Cellular Biology (IGBMC), Centre National de la Recherche Scientifique/Institut National de la Santé et de la Recherche Médicale/University of Strasbourg, Strasbourg, France,

⁶Department of Surgery and Centre of Minimally Invasive Surgery, Evangelische Kliniken Essen-Mitte, Academic Teaching Hospital of the University of Duisburg-Essen, Essen, Germany, and ⁷First Propaedeutic Department of Internal Medicine, Laikon Hospital, National and Kapodistrian University of Athens, and ⁸Department of Pathology, 'G. Gennimatas' Athens General Hospital, Athens, Greece

Correspondence to: Dr B. Seeliger, IHU-Strasbourg, 1 Place de l'Hôpital, 67091 Strasbourg Cedex, France (e-mail: barbara.seeliger@ihu-strasbourg.eu;

 @IHUStrasbourg, @IrcadFrance, @_kem, @unistra, @CHRUStrasbourg, @IGBMC)

Background: A surgical approach preserving functional adrenal tissue allows biochemical cure while avoiding the need for lifelong steroid replacement. The aim of this experimental study was to evaluate the impact of intraoperative imaging during bilateral partial adrenalectomy on remnant perfusion and function.

Methods: Five pigs underwent bilateral posterior retroperitoneoscopic central adrenal gland division (9 divided glands, 1 undivided). Intraoperative perfusion assessment included computer-assisted quantitative fluorescence imaging, contrast-enhanced CT, confocal laser endomicroscopy (CLE) and local lactate sampling. Specimen analysis after completion adrenalectomy (10 adrenal glands) comprised mitochondrial activity and electron microscopy.

Results: Fluorescence signal intensity evolution over time was significantly lower in the cranial segment of each adrenal gland (mean(s.d.) 0.052(0.057) versus 0.133(0.057) change in intensity per s for cranial versus caudal parts respectively; $P = 0.020$). Concordantly, intraoperative CT in the portal phase demonstrated significantly lower contrast uptake in cranial segments ($P = 0.031$). In CLE, fluorescein contrast was observed in all caudal segments, but in only four of nine cranial segments ($P = 0.035$). Imaging findings favouring caudal perfusion were congruent, with significantly lower local capillary lactate levels caudally (mean(s.d.) 5.66(5.79) versus 11.58(6.53) mmol/l for caudal versus cranial parts respectively; $P = 0.008$). Electron microscopy showed more necrotic cells cranially ($P = 0.031$). There was no disparity in mitochondrial activity (respiratory rates, reactive oxygen species and hydrogen peroxide production) between the different segments.

Conclusion: In a model of bilateral partial adrenalectomy, three intraoperative imaging modalities consistently discriminated between regular and reduced adrenal remnant perfusion. By avoiding circumferential dissection, mitochondrial function was preserved in each segment of the adrenal glands.

Surgical relevance

Preservation of adrenal tissue to maintain postoperative function is essential in bilateral and hereditary adrenal pathologies. There is interindividual variation in residual adrenocortical stress capacity, and the minimal functional remnant size is unknown.

New intraoperative imaging technologies allow improved remnant size and perfusion assessment. Fluorescence imaging and

contrast-enhanced intraoperative CT showed congruent results in evaluation of perfusion.

Intraoperative imaging can help to visualize the remnant vascular supply in partial adrenalectomy. Intraoperative assessment of perfusion may foster maximal functional tissue preservation in bilateral adrenal pathologies and procedures.

Presented in part to the 106th Annual Congress of the Swiss Society of Surgery, Berne, Switzerland, May 2019, and will be presented to the 9th Biennial Congress of the European Society of Endocrine Surgeons, Athens, Greece, May 2021; published in abstract form as *Br J Surg* 2020; 107(Suppl 2): 6

Paper accepted 31 May 2020

Published online 1 September 2020 in Wiley Online Library (www.bjs.co.uk). DOI: 10.1002/bjs.11839

Introduction

Cortical-sparing surgery is a surgical approach in which functional adrenal tissue is preserved, unilaterally or bilaterally, whenever possible. In primary adrenal pathologies, it allows biochemical cure while avoiding the need for life-long steroid replacement. Cortical-sparing surgery results in low rates of adrenal insufficiency and disease recurrence, as demonstrated for various unilateral and bilateral adrenal neoplasias^{1–4}. The retroperitoneoscopic approach has been reported to be associated with the lowest recurrence rates after partial adrenalectomy⁵. An increasing number of small adrenal masses has been identified through the widespread use of imaging modalities. Adrenal-sparing surgery is gaining popularity worldwide⁶, and removal of the entire gland can no longer be recommended as the standard treatment for small benign adrenal tumours⁷. Preservation of functional adrenal tissue has to be pursued for bilateral tumours, and may be considered for unilateral disease if the lesion can be removed completely⁸.

Optimal perfusion is key to the preservation of organ function. Advances in intraoperative imaging technologies have led to the potential for precise assessment of organ perfusion⁹. Not only does CT determine adrenal remnant volume¹⁰, but its intraoperative use with contrast enhancement can also provide perfusion assessment. Imaging based on fluorescence angiography allows quantification of organ perfusion in real time. Confocal laser endomicroscopy (CLE) enables evaluation of the microcirculation, in addition to real-time *in vivo* histopathological assessment⁹.

The aim of this study was to investigate whether postoperative remnant adrenal function can be estimated using intraoperative imaging technologies, in a model of cortical-sparing bilateral posterior retroperitoneoscopic adrenal surgery.

Methods

Five Large White pigs (*Sus scrofa domesticus*, four male and one female; mean(s.d.) weight 42.8(3.9) kg) were used in the study, as part of the ELIOS (Endoscopic Luminescent Imaging for precision Oncologic Surgery) protocol, which received full approval from the local Ethical Committee on Animal Experimentation (ICOMETH 38.2017.01.085), and the Ministry of Superior Education and Research (APAFIS 8721-2017013010316298v2). All animals used in the experimental laboratory were managed according to French laws for animal use and care, European Community Council directives (2010/63/EU), and ARRIVE guidelines, as described previously¹¹.

To reduce the number of animals used, a bilateral approach simulating four adrenal remnants per pig was

chosen. The animals underwent posterior retroperitoneoscopic central division of both adrenal glands (9 divided glands, 1 intact gland). Intraoperative tools for remnant perfusion assessment included computer-assisted quantitative fluorescence imaging, local lactate sampling, contrast-enhanced CT and CLE. After bilateral retroperitoneoscopic completion adrenalectomy (10 glands), specimen analysis included mitochondrial activity and electron microscopy on surgical biopsies of all four regions of interest (ROIs).

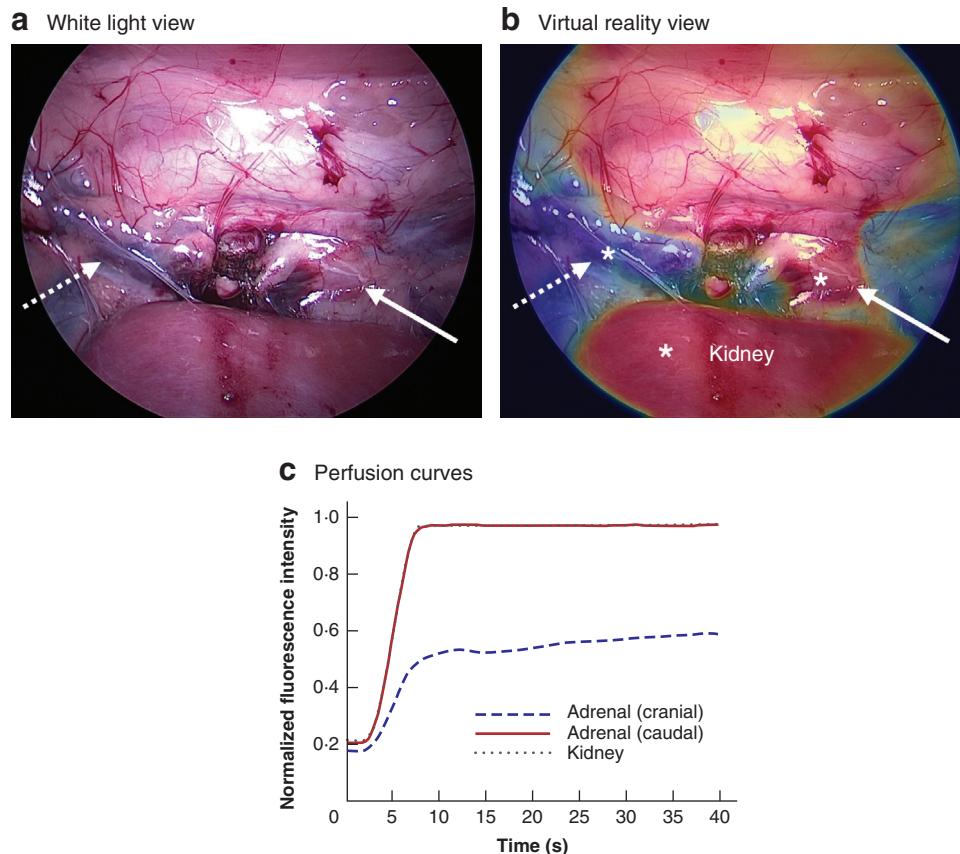
Operative technique

The operative technique described for posterior retroperitoneoscopic adrenalectomy in the porcine model¹² was derived from the human technique². As a partial adrenalectomy model of four adrenal segments per pig, bilateral central division of each gland created a cranial and a caudal remnant on each side. A vessel-sealing device was used (LigaSure™; Medtronic, Minneapolis, Minnesota, USA) for gland division without circumferential dissection. With this bilateral retroperitoneoscopic access, simultaneous adrenal fluorescence imaging was done by intravenous administration of 3 ml of a 2.5-mg/ml indocyanine green (ICG) solution (Infracyanine®; Serb, Paris, France), using two near-infrared camera systems (D-LIGHT P; Karl Storz, Tuttlingen, Germany)¹². After intraoperative imaging and lactate analyses, completion adrenalectomy was performed. The adrenal glands were extracted through a port, and subjected to postoperative specimen analysis.

Intraoperative analysis

Fluorescence-based enhanced reality computer-assisted fluorescence imaging

Fluorescence-based enhanced reality (FLER) imaging was done using ER-PERFUSION software to simultaneously and quantitatively analyse perfusion in all adrenal gland segments. This proprietary software, developed at the Institute for Research against Digestive Cancer (IRCAD) France¹³, measures the dynamic evolution of fluorescence signal intensity (FSI) over time. Focusing on the 40-s time interval between FSI arrival and signal decrease, the variation from 25 to 75 per cent of maximal intensity was analysed. This slope of FSI evolution dynamics was used for quantitative near-infrared fluorescence perfusion imaging^{11,12}. Perfusion data from each imaging system were translated into a colour-coded cartogram, which was superimposed on to the real-time view of the corresponding left and right camera systems¹².

Fig 1 Quantitative adrenal perfusion assessment using fluorescence-based enhanced reality computer-assisted fluorescence imaging

a White light and **b** enhanced reality intraoperative views of a divided left adrenal gland. Asterisks mark measuring points for representative perfusion curves. **c** Perfusion curves for cranial and caudal parts of the adrenal gland, and kidney. The cranial adrenal part (dotted arrow) shows decreased perfusion (blue), whereas perfusion of the caudal segment (solid arrow, red) is equal to that of the kidney.

Intraoperative CT

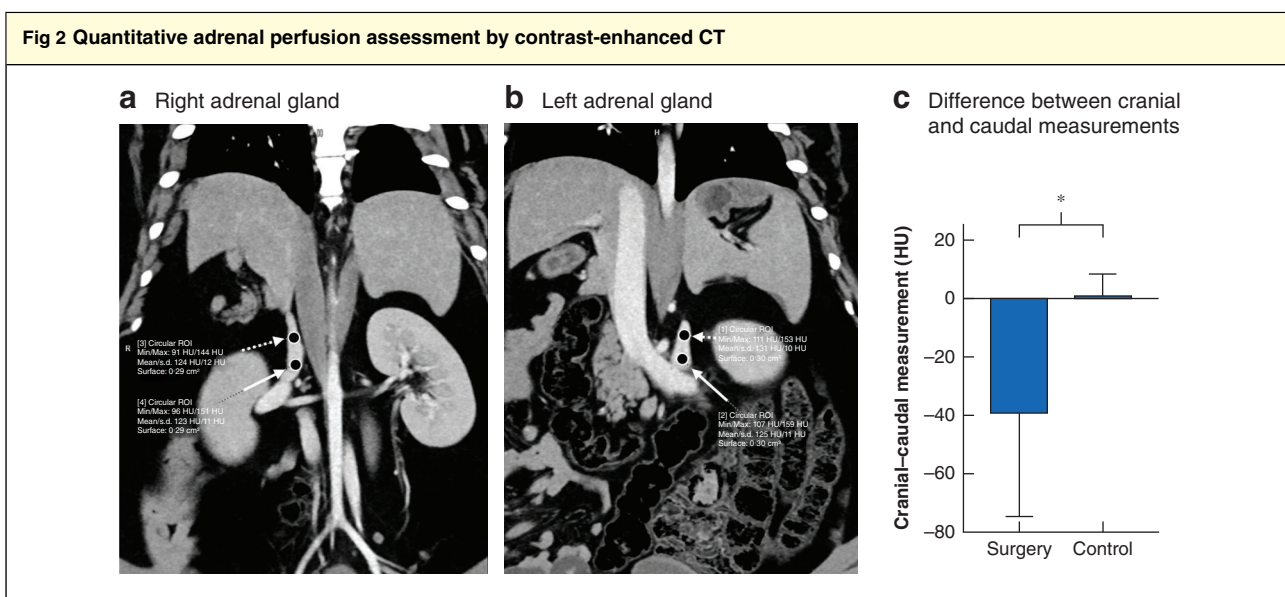
Dual-phase abdominal CT was carried out immediately after surgical division of both adrenal glands (Somatom Definition AS; Siemens, Erlangen, Germany) (1 s gantry rotation time, 128×0.6 mm section collimation using a z-flying focal spot, and 700 reference mAmp-s tube current with automatic exposure control at a tube voltage of 100 kV for the arterial phase and 120 kV for the portal phase) following intravenous injection of contrast (50 ml Iomeron[®] 400; Bracco Imaging, Milan, Italy); the arterial-phase scan was acquired 35 s after the start of contrast administration, and the portal-phase scan 80 s after the start of contrast administration.

CT images from three pigs randomly selected from the authors' database (6 adrenal glands without surgical intervention) served as controls for CT perfusion analysis.

Using the portal-phase acquisition, contrast uptake was estimated by placing a 0.3-cm^2 circular ROI cranially and caudally in both adrenal glands. The mean Hounsfield Unit (HU) value within the ROI was considered a surrogate marker of perfusion for the respective gland segment. The difference in HU between cranial and caudal ROIs of each gland was compared between the surgery and control groups.

Confocal laser endomicroscopy

Probe-based CLE was performed on both segments of each adrenal gland, using a GastroFlex[™] UHD Confocal Miniprobe[™] (Cellvizio[®]; Mauna Kea Technologies, Paris, France) as described previously¹⁴. Video recording of adrenal CLE probe imaging was done directly after intravenous injection of 5 ml 10 per cent sodium



CT images of **a** right and **b** left adrenal gland (control group). Regions of interest (ROIs) are marked by black circles; dotted arrows represent the cranial part and solid arrows the caudal part. **c** Mean(s.d.) difference between cranial and caudal CT measurements in surgery and control groups. HU, Hounsfield Units. * $P = 0.006$ (Mann–Whitney U test).

fluorescein (Fluocyne®; Serb). The presence or absence of fluorophore arrival in the tissue was documented.

Lactate measurement

Adrenal capillary blood samples were obtained by puncturing the ROIs in each gland one by one, sterile aspiration through a trocar using a motorized pipette filler, and analysis using a strip-based EDGE Blood Lactate Monitoring System (ApexBio, Hsinchu City, Taiwan)¹¹.

Postoperative specimen analysis

Additional technical details can be found in *Appendix S1* (supporting information).

Electron microscopy

The ultrastructural analysis focused on the zona fasciculata, which forms up to 75 per cent of the adrenal cortex and is the principal source of glucocorticoid hormone synthesis that is essential for life¹⁵. Semithin sections were examined using an optical microscope, and ultrathin sections using an electron microscope.

Mitochondrial respiratory chain assessment and hydrogen peroxide production

In biopsies obtained immediately after surgical removal of each specimen, mitochondrial respiratory rate was measured by a technique reported elsewhere¹⁶, and hydrogen peroxide production was determined simultaneously

using a high-resolution oxygraph (Oxygraph-2 k; Oroboros Instruments, Innsbruck, Austria).

Determination of reactive oxygen species formation

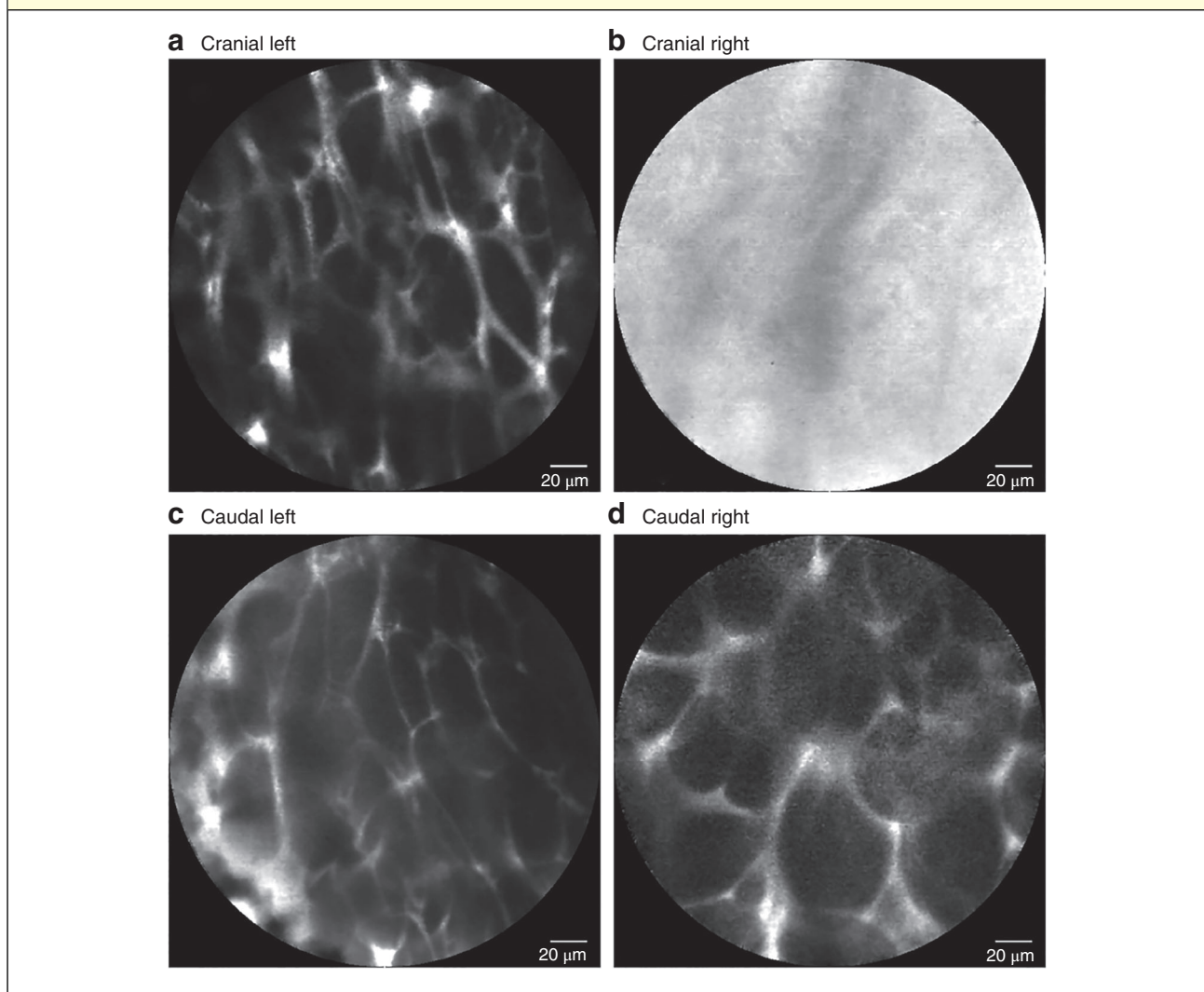
By detecting and recording electromagnetic radiation energy, the reactive oxygen species (ROS) concentration was determined directly with a specific spin probe (1-hydroxy-3-methoxycarbonyl-2,2,5,5-tetramethylpyrrolidine hydrochloride)¹⁷.

Statistical analysis

The sample size was calculated based on a previous study of bowel ischaemia¹³. Eight control adrenal biopsies for mitochondrial function assessment were obtained within the framework of another study, immediately after induction of anaesthesia. Using a superiority design, and based on the hypothesis that the maximum mitochondrial respiratory rate (V adenosine 5'-diphosphate (ADP)) decrease in the experimental group would be at least 60 per cent compared with that in the control group, a sample size of six assessment points per group was deemed sufficient to detect a significant difference with an α of 5 per cent and a power $(1 - \beta)$ of 90 per cent.

To compare values for the cranial and caudal segments of each gland, the Wilcoxon matched-pairs signed-rank test was used for analyses of CT, FLER, lactate concentration, necrosis rate and mitochondrial function, and the

Fig 3 Confocal laser endomicroscopic image series from one animal



After adrenal gland division, both a cranial and c caudal left adrenal gland segments and the d right caudal one remained vascularized, with fluorescein contrast enhancement in the abundant capillary network. b No contrast enhancement was observed in the right cranial segment owing to insufficient arterial inflow.

χ^2 test with Yates' correction for analysis of CLE data. The Mann–Whitney U test was used to compare measurements between the control and surgery groups in the analysis of CT values. $P < 0.050$ was considered statistically significant. All statistical analyses were done using Prism[®] version 8 for macOS[®] (GraphPad Software, San Diego, California, USA).

Results

Retroperitoneoscopic access and bilateral adrenal gland division, intraoperative imaging and subsequent

adrenalectomies were completed without complications using three trocars on each side and an insufflation pressure of 12–15 mmHg.

Fluorescence-based enhanced reality computer-assisted fluorescence imaging

Perfusion as the speed of fluorescence signal arrival is represented by FSI variation over time, calculated using FLER. As the D-LIGHT P imaging system uses an eight-bit code (scale range 0 (no signal) to 255 (maximum intensity)), the measured FSI values were normalized

(divided by 255, resulting in a range from 0 to 1). As the video records one frame every 0.2 s, division by 0.2 resulted in data expression as the slope of normalized fluorescence intensity variation over time, in ΔI per s. The slope was significantly lower in the cranial than in the caudal segment of each adrenal gland (mean(s.d.) 0.052(0.057) *versus* 0.133(0.057) $\Delta I/s$; $P = 0.020$). Superimposition of the ER-PERFUSION software-based colour-coded perfusion cartogram provided an enhanced reality view in real time (Fig. 1).

Contrast-enhanced CT

Intraoperative CT demonstrated significantly lower contrast uptake in cranial compared with caudal segments in the portal phase ($P = 0.031$). The mean difference between cranial and caudal contrast uptake was significantly greater in the surgery group than in the control group (mean(s.d.) $-39.14(35.57)$ *versus* $1.29(7.25)$ HU; $P = 0.006$) (Fig. 2).

Confocal laser endomicroscopy

Although fluorescein contrast was observed in all caudal segments, it was present in only four of nine cranial segments ($P = 0.035$) (Fig. 3).

Local adrenal capillary lactate levels

Local capillary lactate levels were significantly higher in the cranial than in the caudal adrenal segment (mean(s.d.) $11.58(6.53)$ *versus* $5.66(5.79)$ mmol/l respectively; $P = 0.008$).

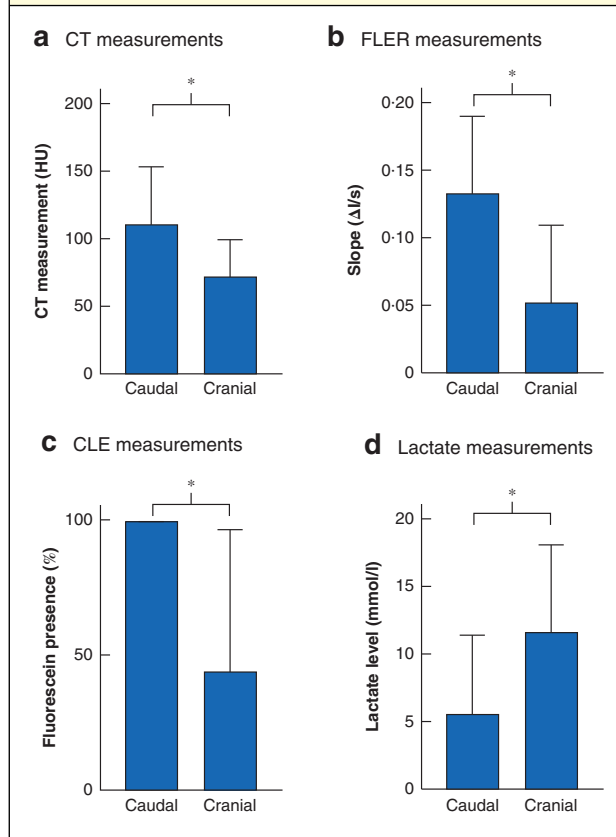
Overview of *in vivo* analyses

Intraoperative discrimination between regular and reduced perfusion of adrenal remnants was achieved using diverse imaging modalities. This *in vivo* analysis showed concordant quantitative findings for perfusion evaluation by means of FLER fluorescence imaging and contrast-enhanced CT. They were also consistent with CLE observations, and validated by the intraoperative metabolic assessment using local capillary lactate levels, which favoured caudal segment perfusion (Fig. 4).

Electron microscopy

Representative toluidine blue-stained semithin sections and electron microscopic images of bilateral gland segments from one pig are shown in Fig. S1 (supporting information). Histopathological and ultrastructural features are detailed in Appendix S2 (supporting information).

Fig 4 Comparison of results for different intraoperative assessment modalities

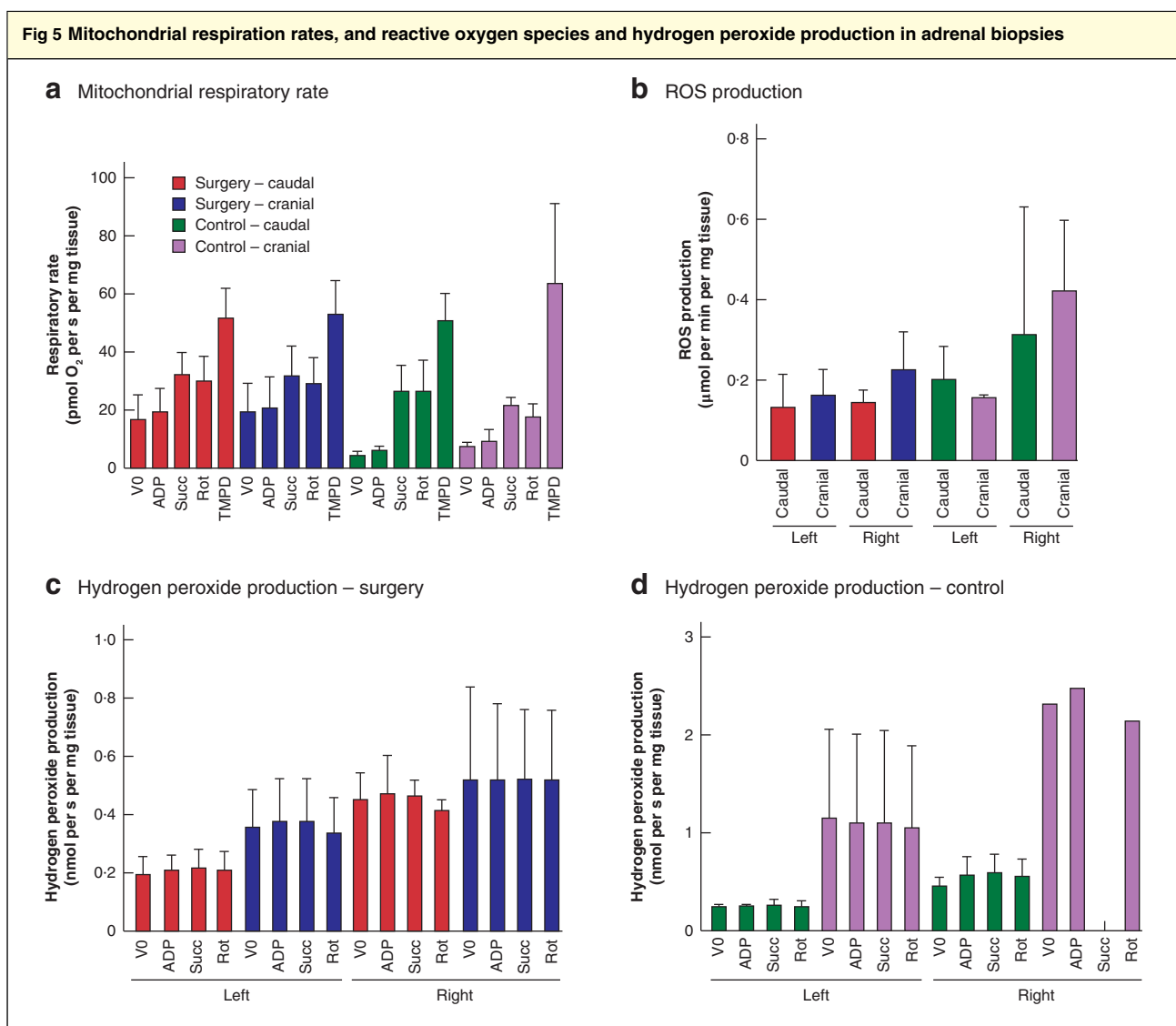


Measurements from **a** CT, **b** fluorescence-based enhanced reality (FLER) computer-assisted fluorescence imaging and **c** confocal laser endomicroscopy (CLE), and **d** local capillary lactate concentration. The higher uptake of contrast in caudal segments shown by CT, FLER and CLE was indicative of the preserved arterial blood supply in this region. With reduced oxygen supply due to impaired arterial inflow, lactate production was increased in cranial segments. HU, Hounsfield Units; ΔI , change in intensity. Values are mean(s.d.). * $P < 0.050$ (a,b,d Wilcoxon matched-pairs signed-rank test; c χ^2 test with Yates' correction).

More necrotic cells were observed in cranial segments than caudal ones ($41.1(27.6)$ *versus* $14.4(7.3)$ per cent; $P = 0.031$). In the majority of remnants (16 of 19), the cellular necrosis rate determined using electron microscopy was 50 per cent or less.

Mitochondrial respiratory chain assessment

Mitochondrial respiration rates did not differ between cranial and caudal segments, either after gland division, or in the control group. In an analysis according to time interval between gland division and specimen extraction with biopsies (range 1.75–4.3 h), there was no statistically significant time-dependent difference (less than 3 h



a Mitochondrial respiratory rate, **b** reactive oxygen species (ROS) production, and **c,d** hydrogen peroxide production in surgery (**c**) and control (**d**) groups. Values are mean(s.d.). V0, basal oxygen consumption; ADP, adenosine 5'-diphosphate; Succ, succinate; Rot, rotenone; TMPD, *N'*-tetramethyl-*p*-phenylenediamine dihydrochloride.

versus 3 h or more). Basal and maximum oxygen consumption were significantly higher in the surgery group than in the control group (V0 and V ADP both $P < 0.001$), including respiratory rate in the presence of succinate ($P = 0.042$). Mitochondrial respiratory rates after stimulation of complex IV (respiratory rate after addition of *N'*-tetramethyl-*p*-phenylenediamine dihydrochloride and ascorbate) were maintained in all segments. (Fig. 5a). The residual perfusion after gland division preserved mitochondrial activity, as demonstrated by a physiological response to all added substrates for the different mitochondrial complexes.

Hydrogen peroxide production

No significant difference in hydrogen peroxide production rates was observed between groups (surgery *versus* control, interval less than 3 h *versus* 3 h or more) or different segments (Fig. 5c,d).

Reactive oxygen species formation

There was no statistically significant difference in ROS production between the groups or different segments (Fig. 5b). Comparing corresponding ROIs, there was a

non-significant tendency towards higher ROS production in the control group. A significantly higher ROS production rate was observed for an interval between gland division and specimen biopsies of 3 h or more *versus* less than 3 h (0.18(0.07) *versus* 0.12(0.06) $\mu\text{mol per min per mg dry weight}$ respectively; $P = 0.050$).

Overview of *ex vivo* analyses

Electron microscopy identified signs of cellular damage in some cranial adrenal segments. However, as visualized by mitochondrial respirometry (Fig. S2, supporting information), the functional capacity of each segment was preserved in the surgery group. Tendencies towards higher hydrogen peroxide and ROS production in the right *versus* left and cranial *versus* caudal ROIs did not reach statistical significance.

Discussion

The present study was based on the ability of quantitative fluorescence imaging to visualize adrenal perfusion¹². FLER was complemented by further quantitative measurements from contrast-enhanced CT (contrast uptake in adrenal segments) and local capillary lactate levels, along with the binary interpretation of CLE (presence or absence of fluorescein uptake). Contrast-enhanced intraoperative CT is feasible where available, but entails exposure to ionizing radiation and has a significant impact on surgical workflow⁹. Fluorescence imaging is more practicable. Probe-based CLE was able to visualize preserved arterial perfusion with fluorescein uptake, whereas FLER allowed quantification of the speed of fluorescence signal arrival.

After gland division, all intraoperative measurements concordantly discriminated between regular and reduced adrenal remnant perfusion. The cranial adrenal segment was at higher risk of venous congestion and arterial perfusion deficiency, with division of the main vascular supply (dominant caudal arteries and caudal outlet of central veins). Although the right adrenal vein is located near the superior pole in humans, the porcine one drains caudally into the vena cava. On the left side, in both species the central adrenal vein drains caudally into the left renal vein¹² (Fig. S3, supporting information). Consequently, venous congestion was observed in the opposite pole of each adrenal gland. However, preservation of the main adrenal vein is not required to maintain adrenocortical function^{4,12}. The three groups of arteries (superior/cranial, middle and inferior/caudal) are congruent in the porcine model as well as in humans, as shown in a preparatory study¹² (Fig. S3,

supporting information). Many arterioles form a capsular plexus and irrigate the adrenal cortex¹⁵.

In the present study, reduced perfusion was observed in the cranial segments bilaterally on intraoperative imaging, along with higher lactate levels. These findings can be attributed to a reported dominant supply by the porcine inferior adrenal arteries¹². The abundant arterial network reaching the adrenal capsule has to be preserved in partial adrenalectomy, in order to maximize remnant viability and functionality. Therefore, an optimal surgical technique avoids circumferential dissection in partial adrenalectomy.

Mitochondrial respiratory chain assessment was used to investigate the surgical impact of partial adrenalectomy on steroidogenic function. Quantitative functional estimation of the various mitochondrial enzyme complexes implicated in oxidative phosphorylation, by means of oxygraphic mitochondrial respiratory chain assessment, is a robust tool that has been used in ischaemia–reperfusion studies¹⁸. Significant reductions in basal (V0) and maximum (V ADP) respiratory rate were indicative of early significant respiratory chain impairment in ischaemic zones compared with vascularized zones¹⁸. However, V0 and V ADP were not reduced in the present study, suggesting an absence of significant ischaemic adrenal impairment.

Oxidative stress leads to impaired steroidogenesis, oxidative damage to the adrenal gland, and has been implicated in human adrenal failure¹⁹. Surgical reduction of adrenal size has a negative effect on oxidative stress capacity. Interindividual variation in the procedure's impact on stress capacity has been observed¹⁰. Given the high lipid turnover in the mitochondria and ROS production during steroidogenesis, the adrenal cortex possesses high levels of antioxidants to maintain redox homeostasis and prevent malfunction¹⁹. At low concentrations, ROS promote cell adaptation to stress conditions, supporting cell survival. Once the cellular antioxidant capacity has been overwhelmed, ROS concentrations may increase dramatically and cause substantial cell damage and cell death²⁰. The bilateral tendency towards higher ROS and hydrogen peroxide production in the cranial segments of divided glands could indicate greater vulnerability of the cranial adrenal remnants to maintenance of steroidogenic function. This difference was, however, not statistically significant.

Cortisol measurements were considered initially and, with the few blood drops emerging after puncturing the gland, it may have been possible technically to obtain a sufficient, yet minimal quantity for laboratory analysis. There are, however, no reference values for total and/or free cortisol levels inside the adrenal gland, and no known correlation with postoperative adrenal function.

To prevent an Addisonian crisis with potentially lethal complications after adrenal surgery, exogenous corticosteroid replacement therapy is mandatory. The management of adrenal insufficiency can be challenging, and alternative curative strategies were sought for decades²¹. Attempts at adrenal autotransplantation in the 1960s were discarded. Allograft transplantation and xenotransplantation as well as stem cell treatments have been explored as potential treatment alternatives²¹. Currently, tissue removal needs to be minimized to obtain maximum adrenal function after surgery. Leaving at least 15–30 per cent of residual adrenal tissue has been reported as a requirement for sufficient function^{6,22}. Some authors^{6,23} have demonstrated that patients who have undergone unilateral adrenalectomy do not respond to stress situations in the same way as normal controls. On the other hand, an intact stress capacity was noted in a patient in whom only 10 per cent of adrenal tissue was preserved, and a correlation between residual volume and adrenocortical stress capacity was reported¹⁰. There are currently no definitive data on the minimum amount of residual adrenal tissue to be left *in situ* to maintain physiological adrenal function^{5,10}. Inability to assess the different adrenal zones and cellular cortisol-producing capacity during surgery was the limiting factor in determining the smallest functional adrenal remnant size. The precision of intraoperative adrenal remnant volume determination was found to be limited compared with that of postoperative CT¹⁰.

Fluorescence guidance in cortical-sparing adrenal surgery is currently being explored. In its first clinical description in 2013²⁴, it was used in three patients before adrenal gland dissection during partial adrenalectomy, to differentiate adrenal masses from normal adrenal tissue. Most studies have reported use of ICG injection before adrenal dissection^{25–27}, or before and during adrenal dissection²⁸, for intraoperative guidance. ICG injection is valued not only for guidance during dissection, but particularly for remnant perfusion assessment in partial adrenalectomy¹² (M. K. Walz, P. F. Alesina and B. Seeliger, unpublished clinical data). Fluorescence signal interpretation is, however, subjective and clinical perfusion data are scarce. One study²⁹ reported unilateral visualization of the preserved remnant blood supply in four robot-assisted partial adrenalectomies. A study³⁰ reporting bilateral ICG remnant perfusion imaging in three patients undergoing bilateral laparoscopic partial adrenalectomy was published recently. Persistent adrenal insufficiency was observed in a patient with only moderate fluorescent bilateral remnant vascularization, whereas normal plasma cortisol levels were found in two patients with bilateral well

vascularized fluorescent remnants. The remnant sizes were not reported.

Clinical studies are required to define the smallest functional remnant size, taking residual gland volume and perfusion into account, as well as structural changes. To make a precise assessment of the surgical impact on adrenal/mitochondrial steroidogenic function, intraoperative quantification of remnant size and perfusion status must be correlated with remaining cellular cortisol production capacity. Residual adrenal tissue cannot yet be assessed ultrastructurally in clinical practice without any further reduction of its size by taking biopsies. Quantitative perfusion imaging has the potential to be a surrogate marker for cellular integrity. A significant difference in FSI dynamics between well vascularized and circumferentially dissected malperfused adrenal segments was shown previously¹². In the present study, FLER was again rapid and reproducible, and the findings of all intraoperative imaging techniques used were congruent. The present preclinical investigations were chosen to gain an initial insight into the relationship between intraoperative perfusion assessment and viability of the adrenal remnant. With a necrosis rate of 50 per cent or less in the majority of remnants, the tendency towards higher hydrogen peroxide and ROS production rates in the cranial ROIs suggests a compensatory increase in mitochondrial activity in the viable cells. Hence, although reduced in the cranial segments, remnant perfusion as quantified by CT and FLER seemed sufficient to maintain steroidogenic function. These findings encourage cortical-sparing surgery, with maximal bilateral preservation of adrenal vascularization and healthy parenchyma, in order to avoid adrenal insufficiency and substitution therapy.

Acknowledgements

The authors thank C. Cers-Meunier for illustrating the adrenal vascular anatomy, and radiology technicians for technical and operative assistance; C. Burel and G. Temporal, professionals in medical English, for their assistance in proofreading the manuscript; and the Association d'aide aux insuffisants respiratoires d'Alsace and Association des Opérés du Cœur et des Vaisseaux à Strasbourg for their participation in high-resolution oxygraph and electron paramagnetic resonance equipment acquisition. Double laparoscopic equipment for this study was kindly supplied by Karl Storz. This work was funded by the ARC Foundation for Cancer Research, within the framework of the ELIOS project. This study was funded by IHU-Strasbourg through French National Agency for Research (ANR) grant 10-IAHU-0002. M.D. is member of the scientific

board of Diagnostic Green, and recipient of a grant from the ARC Foundation for the ELIOS project. J.M. is President of the IRCAD Institute, which is partly funded by Karl Storz and Medtronic.

Open Access funding enabled and organized by Projekt DEAL.

[Correction added on 29 October 2020, after first online publication: Projekt Deal funding statement has been added.]

Disclosure: The authors declare no other conflict of interest.

References

- Lowery AJ, Seeliger B, Alesina PF, Walz MK. Posterior retroperitoneoscopic adrenal surgery for clinical and subclinical Cushing's syndrome in patients with bilateral adrenal disease. *Langenbecks Arch Surg* 2017; **402**: 775–785.
- Walz MK, Peitgen K, Diesing D, Petersenn S, Janssen OE, Philipp T *et al.* Partial *versus* total adrenalectomy by the posterior retroperitoneoscopic approach: early and long-term results of 325 consecutive procedures in primary adrenal neoplasias. *World J Surg* 2004; **28**: 1323–1329.
- Castinetti F, Qi XP, Walz MK, Maia AL, Sanso G, Peczkowska M *et al.* Outcomes of adrenal-sparing surgery or total adrenalectomy in pheochromocytoma associated with multiple endocrine neoplasia type 2: an international retrospective population-based study. *Lancet Oncol* 2014; **15**: 648–655.
- Alesina PF, Hinrichs J, Meier B, Schmid KW, Neumann HP, Walz MK. Minimally invasive cortical-sparing surgery for bilateral pheochromocytomas. *Langenbecks Arch Surg* 2012; **397**: 233–238.
- Nagaraja V, Eslick GD, Edirimanne S. Recurrence and functional outcomes of partial adrenalectomy: a systematic review and meta-analysis. *Int J Surg* 2015; **16**(Part A): 7–13.
- Kaye DR, Storey BB, Pacak K, Pinto PA, Linehan WM, Bratslavsky G. Partial adrenalectomy: underused first line therapy for small adrenal tumors. *J Urol* 2010; **184**: 18–25.
- Colleselli D, Janetschek G. Current trends in partial adrenalectomy. *Curr Opin Urol* 2015; **25**: 89–94.
- Lorenz K, Langer P, Niederle B, Alesina P, Holzer K, Nies C *et al.* Surgical therapy of adrenal tumors: guidelines from the German Association of Endocrine Surgeons (CAEK). *Langenbecks Arch Surg* 2019; **404**: 385–401.
- Mascagni P, Longo F, Barberio M, Seeliger B, Agnus V, Saccomandi P *et al.* New intraoperative imaging technologies: innovating the surgeon's eye toward surgical precision. *J Surg Oncol* 2018; **118**: 265–282.
- Brauckhoff M, Stock K, Stock S, Lorenz K, Sekulla C, Brauckhoff K *et al.* Limitations of intraoperative adrenal remnant volume measurement in patients undergoing subtotal adrenalectomy. *World J Surg* 2008; **32**: 863–872.
- Seeliger B, Agnus V, Mascagni P, Barberio M, Longo F, Lapergola A *et al.* Simultaneous computer-assisted assessment of mucosal and serosal perfusion in a model of segmental colonic ischemia. *Surg Endosc* 2019; <https://doi.org/10.1007/s00464-019-07258-z> [Epub ahead of print].
- Seeliger B, Walz MK, Alesina PF, Agnus V, Pop R, Barberio M *et al.* Fluorescence-enabled assessment of adrenal gland localization and perfusion in posterior retroperitoneoscopic adrenal surgery in a preclinical model. *Surg Endosc* 2020; **34**: 1401–1411.
- Diana M, Noll E, Diemunsch P, Dallemagne B, Benahmed MA, Agnus V *et al.* Enhanced-reality video fluorescence: a real-time assessment of intestinal viability. *Ann Surg* 2014; **259**: 700–707.
- Diana M, Dallemagne B, Chung H, Nagao Y, Halvax P, Agnus V *et al.* Probe-based confocal laser endomicroscopy and fluorescence-based enhanced reality for real-time assessment of intestinal microcirculation in a porcine model of sigmoid ischemia. *Surg Endosc* 2014; **28**: 3224–3233.
- Ovalle WK, Nahirney PC, Netter FH. *Netter's Essential Histology* (2nd edn), Vol. xv. Elsevier/Saunders: Philadelphia, 2013.
- Diana M, Halvax P, Pop R, Schlagowski I, Bour G, Liu YY *et al.* Gastric supply manipulation to modulate ghrelin production and enhance vascularization to the cardia: proof of the concept in a porcine model. *Surg Innov* 2015; **22**: 5–14.
- Noll E, Diana M, Charles AL, Singh F, Gan TJ, Pottecher J *et al.* Comparative analysis of resuscitation using human serum albumin and crystalloids or 130/0.4 hydroxyethyl starch and crystalloids on skeletal muscle metabolic profile during experimental haemorrhagic shock in swine: a randomised experimental study. *Eur J Anaesthesiol* 2017; **34**: 89–97.
- Diana M, Agnus V, Halvax P, Liu YY, Dallemagne B, Schlagowski AI *et al.* Intraoperative fluorescence-based enhanced reality laparoscopic real-time imaging to assess bowel perfusion at the anastomotic site in an experimental model. *Br J Surg* 2015; **102**: e169–e176.
- Prasad R, Kowalczyk JC, Meimaridou E, Storr HL, Metherell LA. Oxidative stress and adrenocortical insufficiency. *J Endocrinol* 2014; **221**: R63–R73.
- Makrecka-Kuka M, Krumschnabel G, Gnaiger E. High-resolution respirometry for simultaneous measurement of oxygen and hydrogen peroxide fluxes in permeabilized cells, tissue homogenate and isolated mitochondria. *Biomolecules* 2015; **5**: 1319–1338.
- Ruiz-Babot G, Hadjidemetriou I, King PJ, Guasti L. New directions for the treatment of adrenal insufficiency. *Front Endocrinol (Lausanne)* 2015; **6**: 70.
- Brauckhoff M, Gimm O, Thanh PN, Bar A, Ukkat J, Brauckhoff K *et al.* Critical size of residual adrenal tissue and recovery from impaired early postoperative adrenocortical function after subtotal bilateral adrenalectomy. *Surgery* 2003; **134**: 1020–1027.
- Nakada T, Kubota Y, Sasagawa I, Yagisawa T, Watanabe M, Ishigooka M. Therapeutic outcome of primary aldosteronism: adrenalectomy *versus* enucleation of

- aldosterone-producing adenoma. *J Urol* 1995; **153**: 1775–1780.
- 24 Manny TB, Pompeo AS, Hemal AK. Robotic partial adrenalectomy using indocyanine green dye with near-infrared imaging: the initial clinical experience. *Urology* 2013; **82**: 738–742.
- 25 DeLong JC, Chakedis JM, Hosseini A, Kelly KJ, Horgan S, Bouvet M. Indocyanine green (ICG) fluorescence-guided laparoscopic adrenalectomy. *J Surg Oncol* 2015; **112**: 650–653.
- 26 Colvin J, Zaidi N, Berber E. The utility of indocyanine green fluorescence imaging during robotic adrenalectomy. *J Surg Oncol* 2016; **114**: 153–156.
- 27 Sound S, Okoh AK, Bucak E, Yigitbas H, Dural C, Berber E. Intraoperative tumor localization and tissue distinction during robotic adrenalectomy using indocyanine green fluorescence imaging: a feasibility study. *Surg Endosc* 2016; **30**: 657–662.
- 28 Arora E, Bhandarwar A, Wagh A, Gandhi S, Patel C, Gupta S et al. Role of indo-cyanine green (ICG) fluorescence in laparoscopic adrenalectomy: a retrospective review of 55 cases. *Surg Endosc* 2018; **32**: 4649–4657.
- 29 Kahramangil B, Kose E, Berber E. Characterization of fluorescence patterns exhibited by different adrenal tumors: determining the indications for indocyanine green use in adrenalectomy. *Surgery* 2018; **164**: 972–977.
- 30 Lerchenberger M, Gundogar U, Al Arabi N, Gallwas JKS, Stepp H, Hallfeldt KKJ et al. Indocyanine green fluorescence imaging during partial adrenalectomy. *Surg Endosc* 2020; **34**: 2050–2055.

Supporting information

Additional supporting information can be found online in the Supporting Information section at the end of the article.

